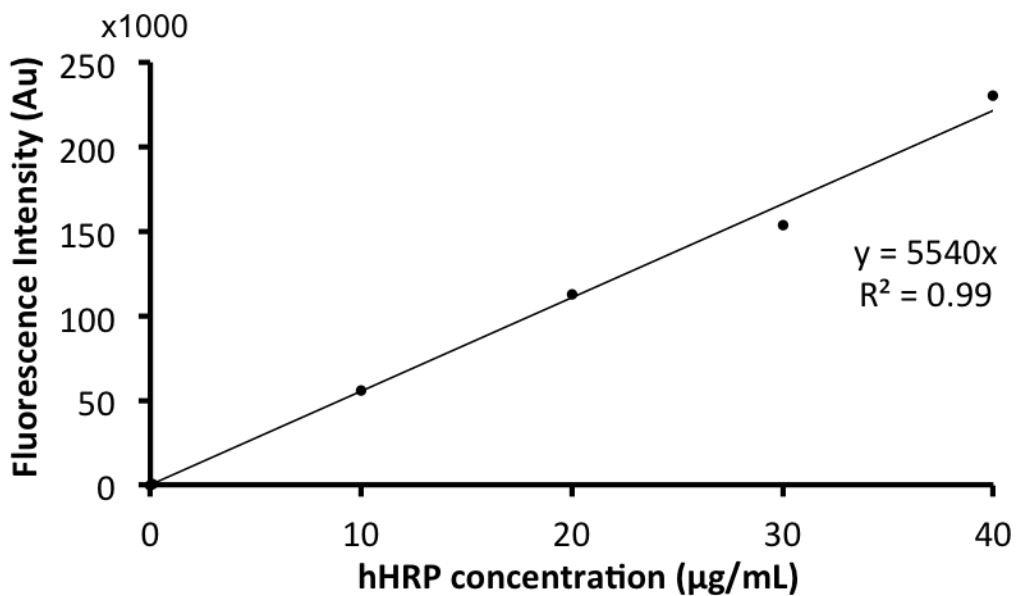


## Porous protein crystals as scaffolds for enzyme immobilization

Ann E. Kowalski, Lucas B. Johnson, Holland K. Dierl, Sehoon Park,  
Thaddaus R. Huber, Christopher D. Snow

### SUPPORTING FIGURES



**Figure S1.** Fluorescence intensity standard curve for concentration of HisProbe™ horseradish peroxidase (hHRP) in Buffer A. Fluorescence measurements were collected on a FLUORstar Omega fluorescence plate reader at 485 nm wavelength excitation.

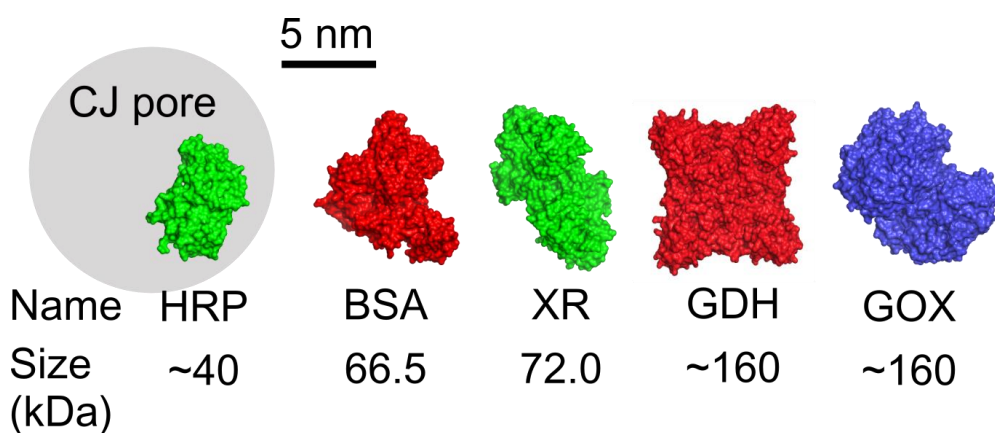


**Figure S2.** Guest proteins loaded in a CJ crystal. From left to right: horseradish peroxidase (HRP), bovine serum albumin (BSA), xylose reductase (XR), glucose dehydrogenase (GDH), glucose oxidase (GOX). Structures based on Protein Data Bank entries 2ATJ, 3V03, 1JEZ, 4MCA, and 1CF3, respectively. Coloring denotes the fluorescent probe used for imaging; the grey circle indicates the average diameter (13 nm) of the central nanopore in CJ crystals. Size estimates are based on the biologically relevant assembly (monomeric for HRP and BSA, dimeric for XR and GOX).

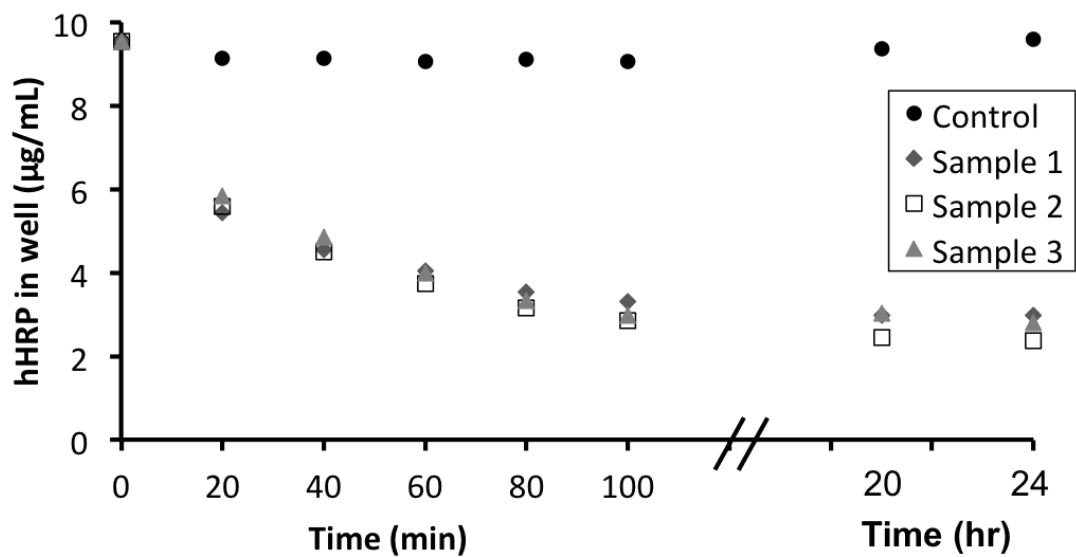


**Figure S3.** Raw hHRP loading data. Each sample consisted of three or more crystals of known volume in a well of 10  $\mu\text{g/mL}$  fluorescently tagged hHRP. As the hHRP loaded into the crystals, a 75  $\mu\text{L}$  aliquot of each sample was extracted to determine the concentration of enzyme remaining in the well using a FluoSTAR Omega fluorescence plate reader with 485 nm wavelength excitation. After each measurement, the 75  $\mu\text{L}$  sample was returned to its well and pipetted to mix with the crystals and remaining solution. A control well showed that the hHRP fluorescence was constant over time in a well that did not contain any crystals.

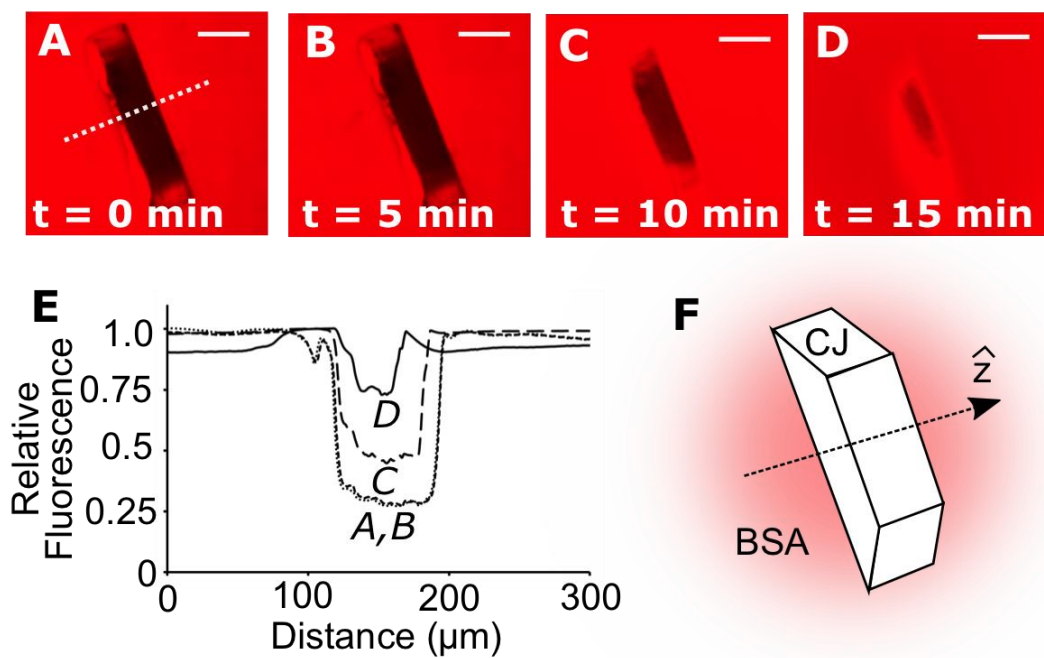


**Figure S4.** BSA diffusion into a crystal. **(A-D)** Time series of BSA loading. The crystal was soaked in 0.1 mg/mL BSA. View is perpendicular to the  $\hat{z}$  axis; scale bar 100  $\mu\text{m}$ . **(E)** Fluorescence intensity profiles measured along the dotted line in A. **(F)** Schematic showing direction of  $\hat{z}$  axis.

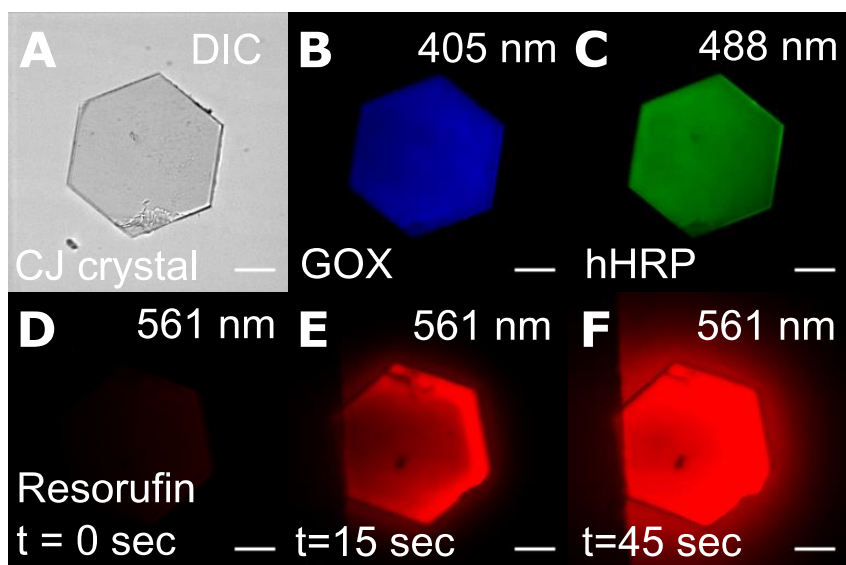


**Figure S5.** GOx/HRP pathway for a non-immobilized CJ crystal. (A) CJ crystal loaded with fluorescently tagged (B) GOx and (C) hHRP. (D-F) Time series of fluorescent resorufin product formation. Scale bars are 100  $\mu\text{m}$ .

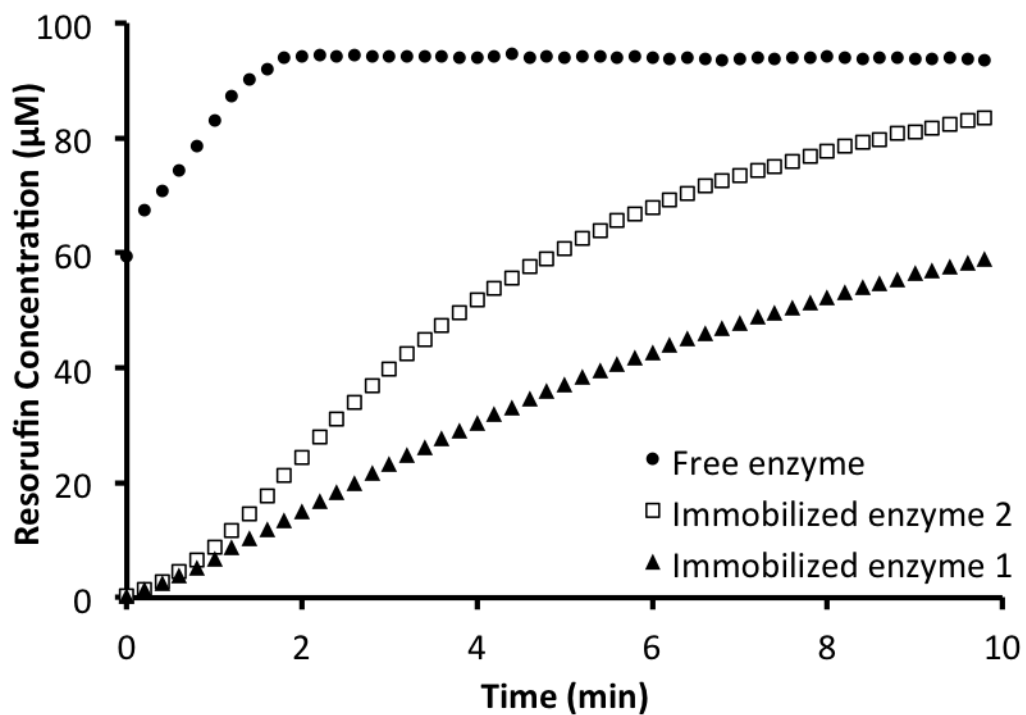
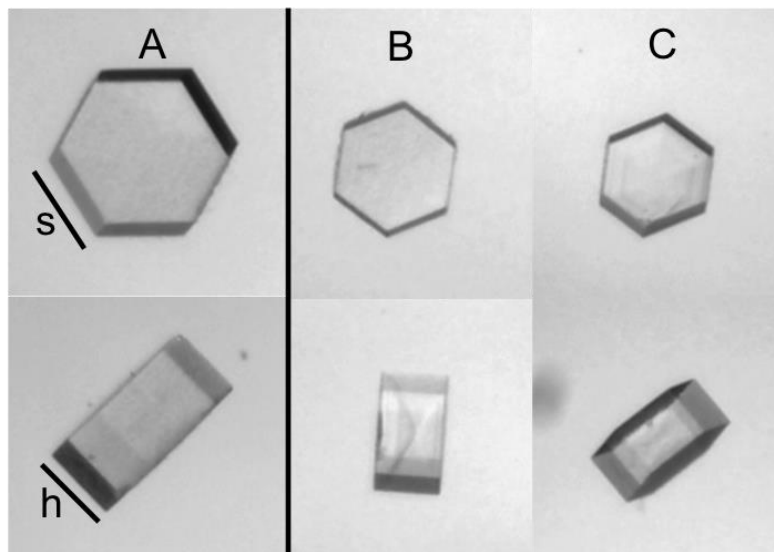


**Figure S6.** A similar experiment to Figure 6 of the main text. Each sample consisted of 0.5 mM hHRP either free in 100 µL of Buffer A or immobilized via Ni(II) affinity within a crystal sample, incubated in 100 µL of Buffer A. The height and volume of Immobilized Enzyme 1 and 2 were 3.1% different, but the surface area of Immobilized Enzyme 2 was 16.8% larger. Each sample was reacted with 100 µM AmplexRed and 100 µM H<sub>2</sub>O<sub>2</sub>.

**Immobilized Enzyme 1**      **Immobilized Enzyme 2**



$$\text{volume (V) of hexagonal prism} = \frac{3\sqrt{3}}{2} s^2 h$$

$$\text{surface area (SA) of hexagonal prism} = 6sh + 3\sqrt{3}s^2$$

$$\begin{aligned} h_A &= h_B = h_C \\ V_A &= V_B + V_C \\ SA_A &> SA_B + SA_C \end{aligned}$$

**Figure S7.** A schematic showing how samples were chosen for the experiments described in Figure 6 and Figure S6. The height of all three crystals in sample 1 and 2 were the same, and the volume of the two crystals in sample 2 was approximately equal ( $\pm 3\%$ ) to that of the one crystal in sample 1. This allowed the same amount of enzyme to be loaded into both samples, but the surface area of sample 2 to be higher than that of sample 1. The surface area is a simple proxy for the idea that enzymes closer to the surface of the crystals will be more productive than enzymes farther in the crystal interior due to transport limitations.

### Crystals used in Figure 6

	Immobilized Enzyme 1	Immobilized Enzyme 2	
s (um)	107.7	93.3	56.3
h (um)	94.0	95.0	76.0
V(um <sup>3</sup> )	2832768.9	2148926.8	625867.3
Total V (um <sup>3</sup> )	2832768.9	2774794.2	
% Difference in V	<b>2.1</b>		
SA (um <sup>2</sup> )	121014.5	98426.6	42143.0
Total SA (um <sup>2</sup> )	121014.5	140569.6	
% Difference in SA	<b>16.2</b>		

### Crystals used in Figure S6

	Immobilized Enzyme 1	Immobilized Enzyme 2	
s (um)	95.9	64.2	69.1
h (um)	74.6	71.2	77.9
V(um <sup>3</sup> )	1782493.4	762433.4	966374.4
Total V (um <sup>3</sup> )	1782493.4	1728807.9	
% Difference in V	<b>3.1</b>		
SA (um <sup>2</sup> )	90712.9	48842.9	57108.0
Total SA (um <sup>2</sup> )	90712.9	105950.9	
% Difference in SA	<b>16.8</b>		

**Table S1.** Description of crystals used in the experiments described in Figures 6 and S6.

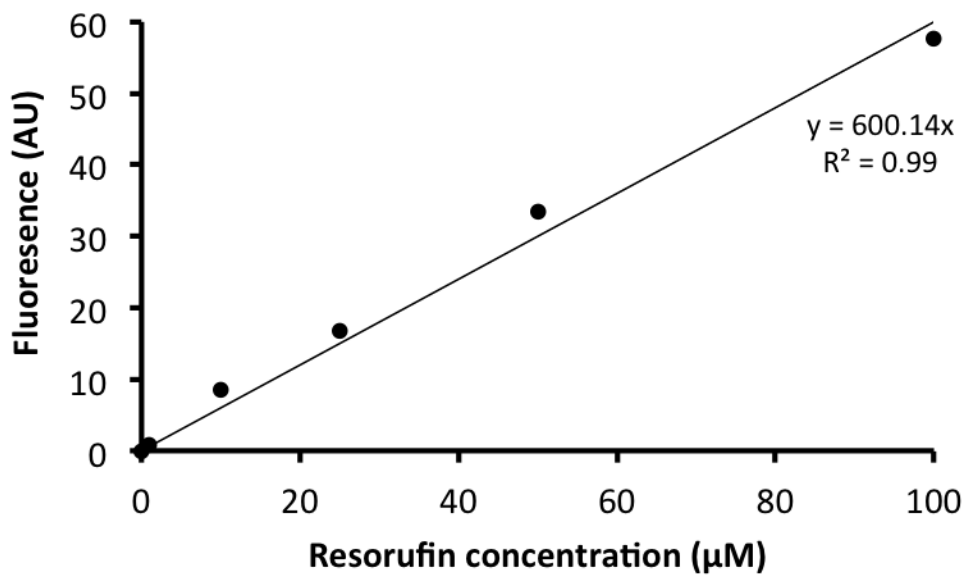


**Figure S8.** Fluorescence intensity standard curve for resorufin in Buffer A. Resorufin is the fluorescent product formed through the oxidation of AmplexRed by hHRP. Fluorescence measurements were collected on a FLUORstar Omega fluorescence plate reader at 561 nm wavelength excitation.

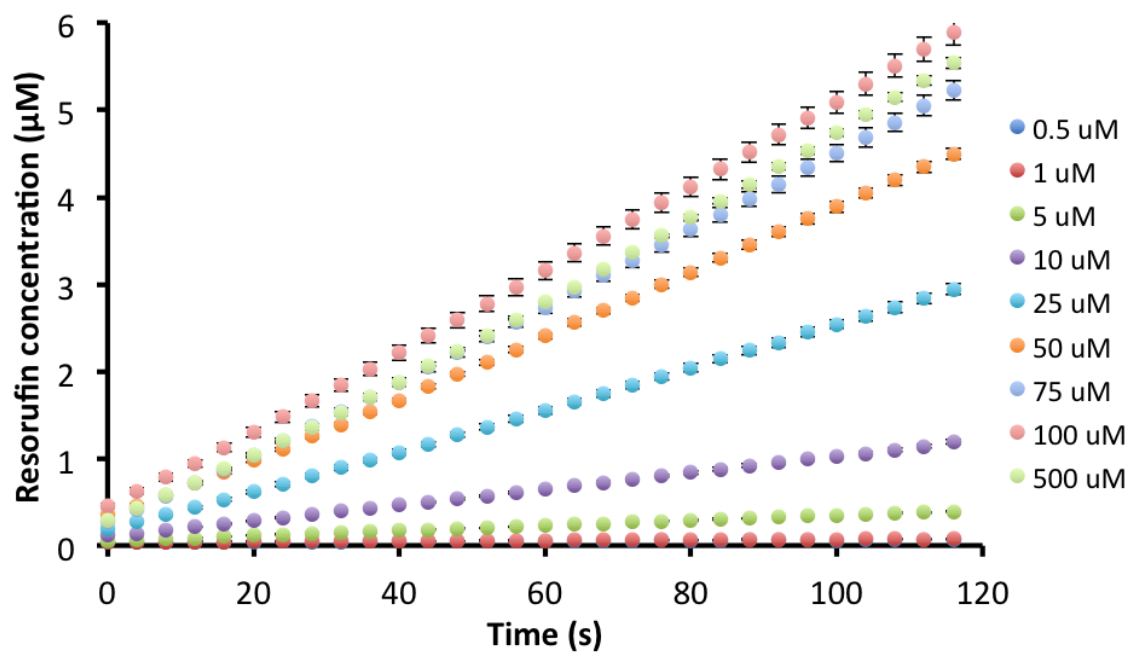


**Figure S9.** Raw activity for free hHRP in Buffer A (0.1 nM) with H<sub>2</sub>O<sub>2</sub> varied from 0.1 - 500 µM and AmplexRed at 100 µM, monitoring fluorescence at 561 nm. Error bars were calculated from the standard deviation of three replicates.

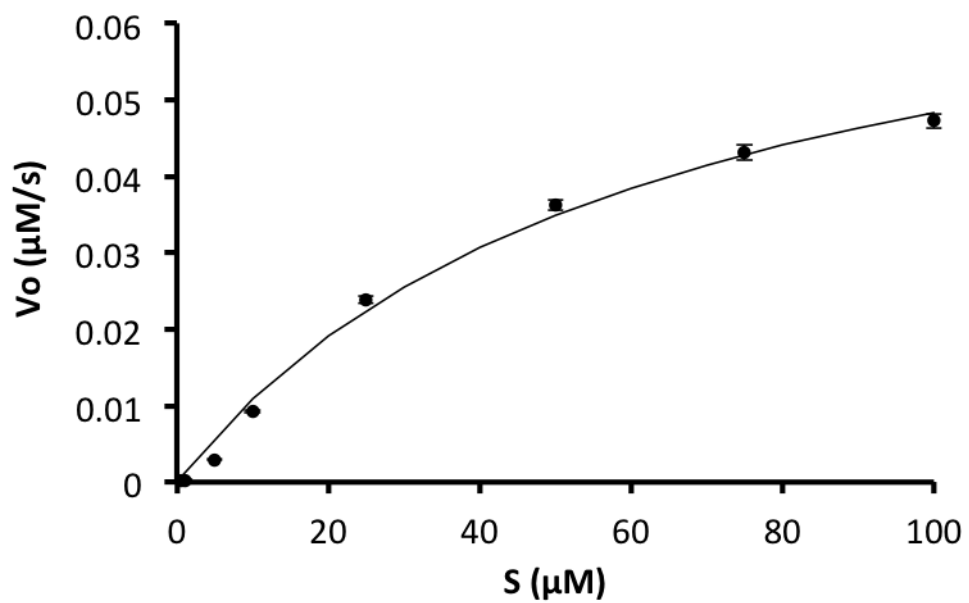


**Figure S10.** Michaelis-Menten plot of the initial rate of resorufin formation as a function of  $\text{H}_2\text{O}_2$  concentration for free hHRP enzyme in solution. Rates calculated from the slope of each line in Figure S9. Errors bars are the standard deviation of triplicate samples.

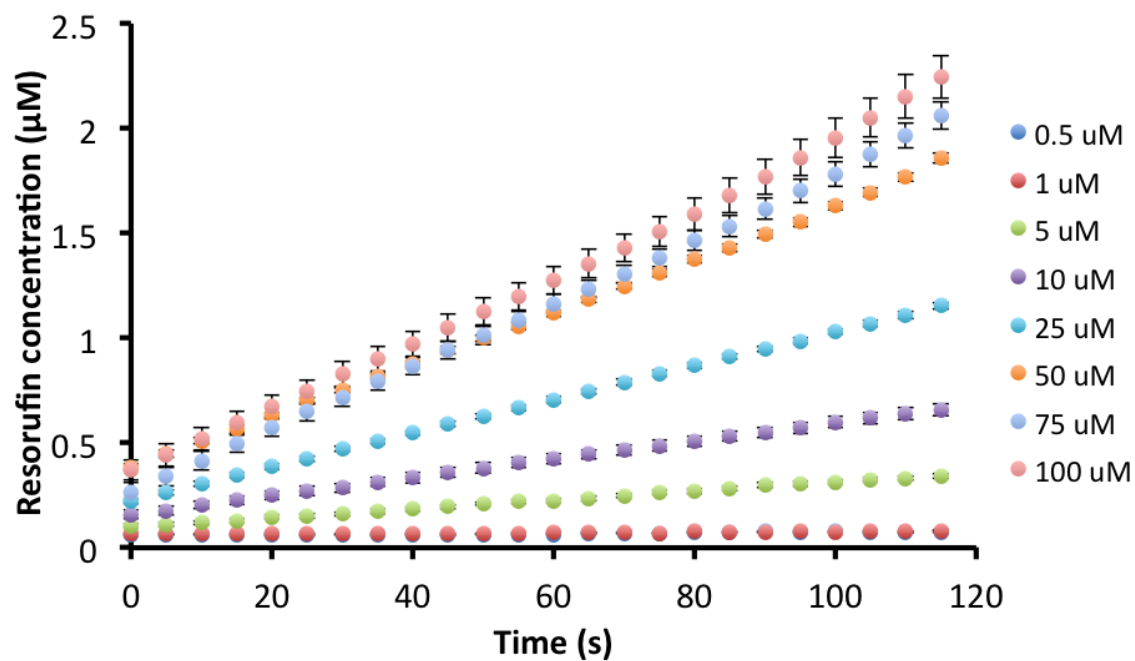


**Figure S11.** Raw activity for microcrystal-immobilized hHRP in Buffer A (0.1 nM) with H<sub>2</sub>O<sub>2</sub> varied from 0.1 - 100 µM and AmplexRed at 100 µM, monitoring fluorescence at 561 nm. Error bars were calculated from the standard deviation of three replicates.

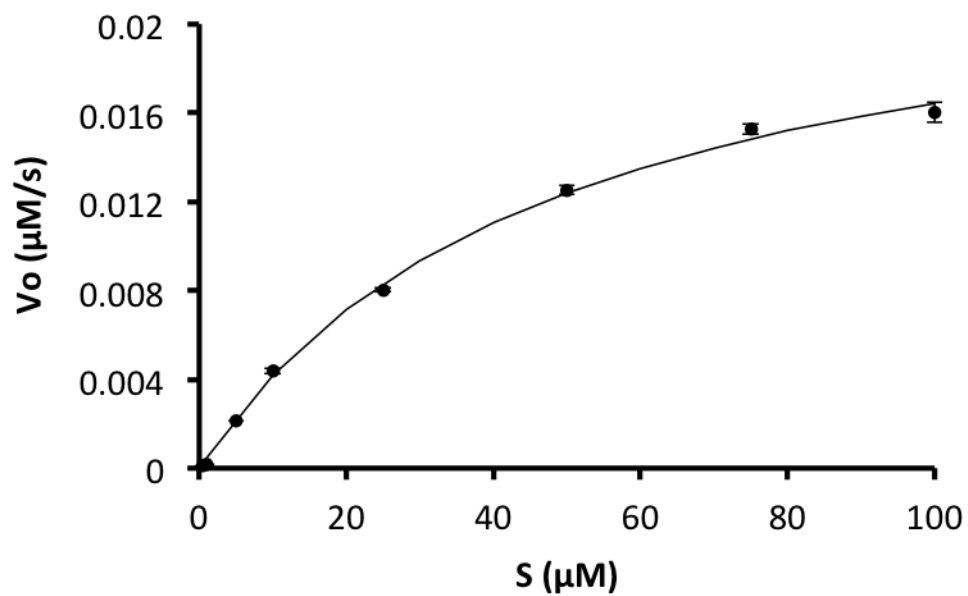


**Figure S12.** Michaelis-Menten plot of the initial rate of resorufin formation as a function of  $\text{H}_2\text{O}_2$  concentration for microcrystal-immobilized hHRP. Rates calculated from the slope of each line in Figure S9. Errors bars are the standard deviation of triplicate samples.

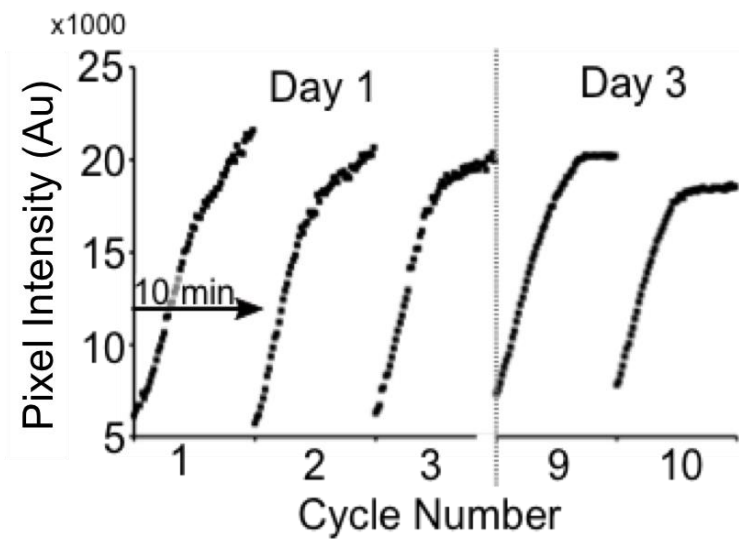


**Figure S13.** Detection of 100  $\mu\text{M}$  glucose in 10 minute GOX/hHRP assays. Enzymes were retained throughout multiple wash/reuse cycles.

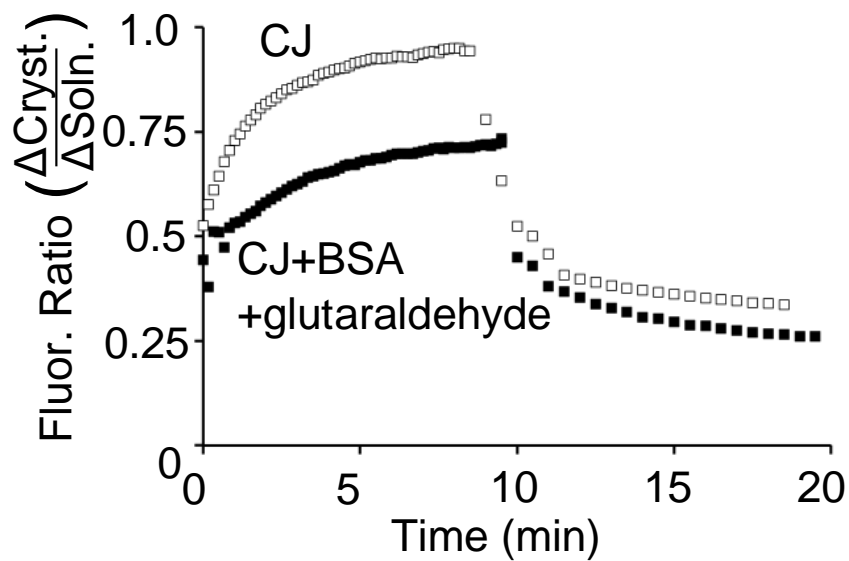


**Figure S14.** Loading and unloading of fluorescently tagged catalase. An empty CJ crystal could readily load catalase as assessed by confocal fluorescence microscopy measured at the crystal midplane. Briefly exposing the crystal to BSA/glutaraldehyde appeared to decrease the loading capacity but did not completely exclude the catalase enzyme.

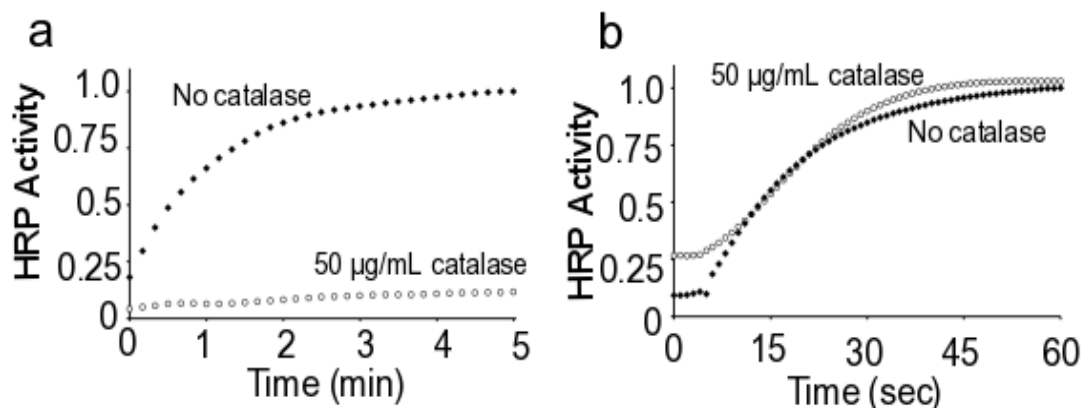


**Figure S15.** Co-immobilizing GOx and hHRP within a BSA/glutaraldehyde-coated protein crystal created a reaction pathway that appeared to be isolated from the surrounding catalase (CAT) enzyme. **(a)** Although CAT drastically decreased hHRP activity (<15% residual activity upon addition of 50 µg/mL CAT) in *in vitro* assays by scavenging the H<sub>2</sub>O<sub>2</sub> intermediate, there was only a minimal change in activity for a GOx/hHRP-laden crystal in CAT-free or 50 µg/mL CAT solutions **(b)**. This result suggested that the H<sub>2</sub>O<sub>2</sub> intermediate was consumed by hHRP within the protein crystal before it was able to diffuse into the surrounding CAT solution, and that CAT was excluded due to the BSA/glutaraldehyde shell. Slight variability in the initial fluorescence was caused by residual bound product from the previous assay. The poor solubility of resorufin may have slowed release from the protein crystal; extensive washing (two or more hours in Buffer A) was required in order to decrease fluorescence to near background levels. The *in vitro* assay was performed on 25 nM GOx, 25 nM hHRP, 50 µM glucose, and 50 µM AmplexRed. Resorufin production was monitored on a fluorescence plate reader at 561 nm excitation.

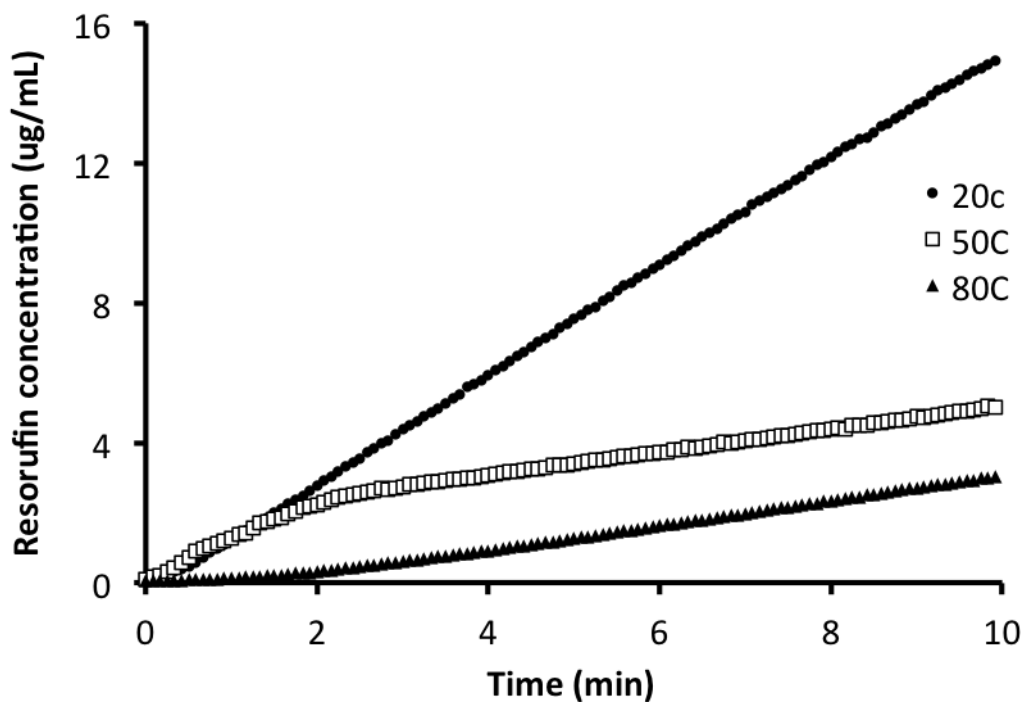


**Figure S16.** Resorufin production from immobilized hHRP enzyme within CJ crystals exposed to  $100 \mu\text{M}$  AmplexRed and  $100 \mu\text{M}$   $\text{H}_2\text{O}_2$ . Crystals were incubated at the specified temperatures for 10 minutes prior to the reaction. The  $80^\circ\text{C}$  and  $50^\circ\text{C}$  crystals were moved to a new drop of Buffer A and allowed to return to room temperature prior to the reaction. Resorufin production was detected at 561 nm wavelength excitation on a fluorescence plate reader.

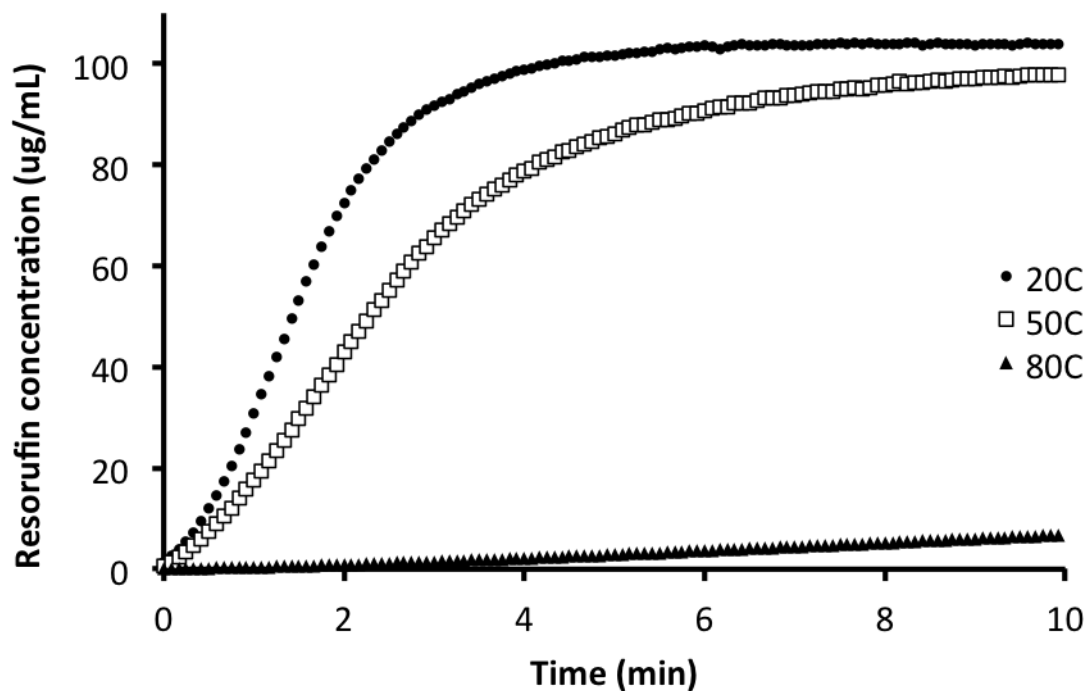


**Figure S17.** Resorufin production from free hHRP enzyme in Buffer A exposed to 100  $\mu\text{M}$  AmplexRed and 100  $\mu\text{M}$   $\text{H}_2\text{O}_2$ . Samples were incubated at the specified temperatures for 10 minutes prior to the reaction. The 80°C and 50°C samples were cooled to room temperature prior to the reaction. Resorufin production was detected at 561 nm wavelength excitation on a fluorescence plate reader.

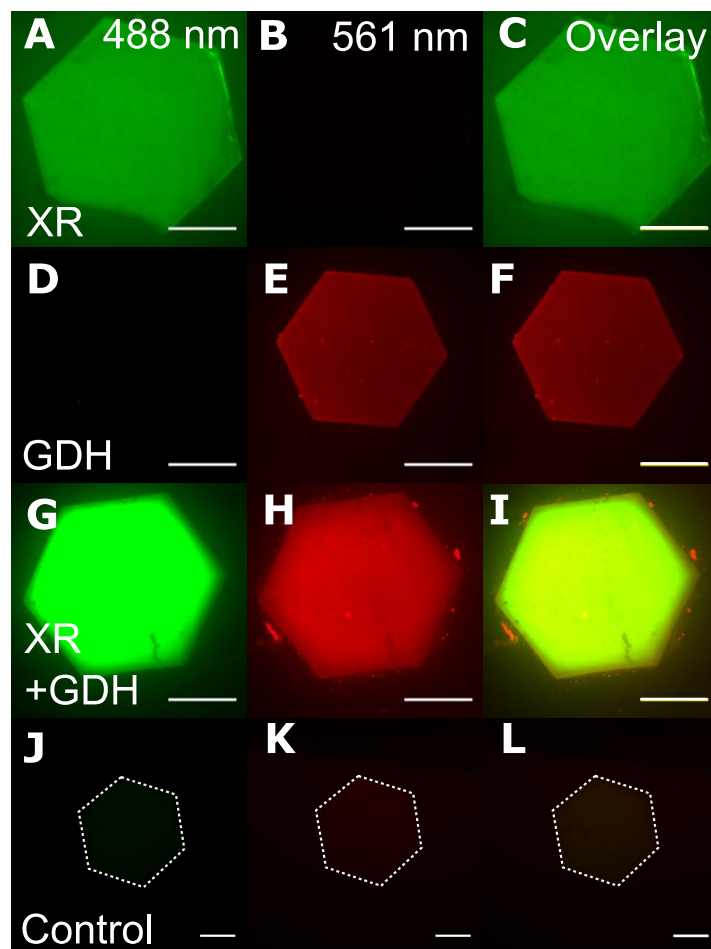


**Figure S18.** Co-immobilization of xylose reductase (XR, green) and glycerol dehydrogenase (GDH, red). (A-C) When XR was loaded individually, fluorescence was only evident at 488 nm wavelength excitation. (D-E) When GDH was loaded individually, fluorescence was only evident at 561 nm wavelength excitation. (G-I) When both enzymes were loaded simultaneously, fluorescence was evident at both wavelengths. (J-L) The fluorescence of an empty control crystal was much lower at both wavelengths. Scale bars are 100  $\mu\text{m}$ .

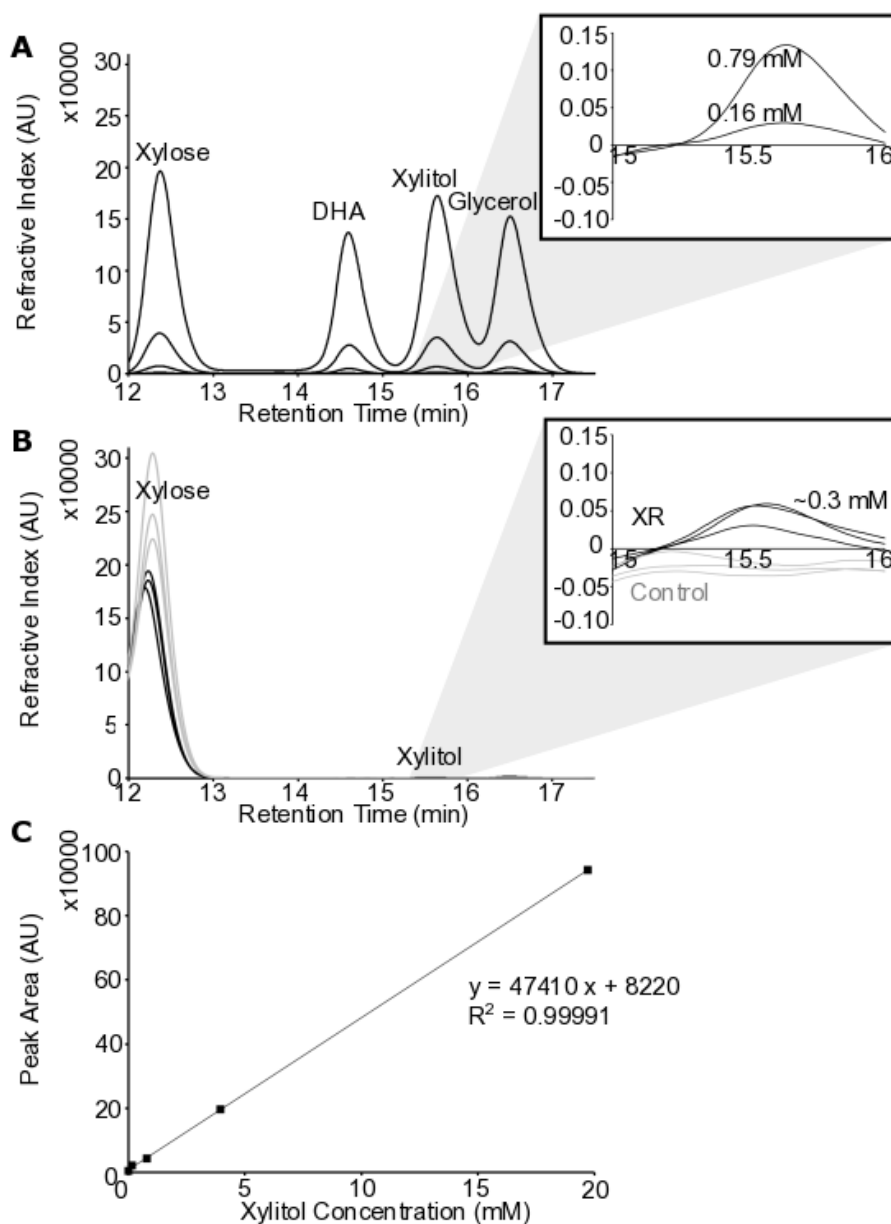


**Figure S19.** Measurement of substrates and products from xylose reductase (XR) assays using HPLC. (A) Overlaid chromatographs for mixtures of xylose, 1,3-dihydroxyacetone, xylitol, and glycerol; the concentration of each component in the mixture was 15, 3, 0.6, 0.12, or 0.024 g/L. Glycerol and 1,3-dihydroxyacetone, the substrate and product of an NADH regenerating glycerol dehydrogenase reaction, were included to ensure peak separation in two-enzyme combined pathways. However, preliminary studies with glycerol dehydrogenase did not show sufficient enzymatic activity to be assessed using HPLC. (Inset) Low range peaks for xylitol standards (0.12 g/L = 0.79 mM, 0.024 g/L = 0.16 mM). (B) Triplicate assays for empty CJ crystals (grey) or CJ crystals loaded with XR (black). Excess xylose substrate was present at the end of each assay. (Inset) Low but measurable concentrations of xylitol were detected in CJ+XR assays but not in empty CJ crystal assays. (C) Standard curve used for estimating xylitol concentration based on peak area.